

Multihadron production features in different reactions

Edward K.G. Sarkisyan^{*,†} and Alexander S. Sakharov^{**,‡}

^{*}*EP Division, Department of Physics, CERN, CH-1211 Geneva 23, Switzerland*

[†]*Department of Physics, the University of Manchester, Manchester M13 9PL, UK*

^{**}*TH Division, Department of Physics, CERN, CH-1211 Geneva 23, Switzerland*

[‡]*Swiss Institute of Technology, ETH-Zürich, 8093 Zürich, Switzerland*

Abstract. We consider multihadron production processes in different types of collisions in the framework of the picture based on dissipating energy of participants and their types. In particular, the similarities of such bulk observables like the charged particle mean multiplicity and the pseudorapidity density at midrapidity measured in nucleus-nucleus, (anti)proton-proton and electron-positron interactions are analysed. Within the description proposed a good agreement with the measurements in a wide range of nuclear collision energies from AGS to RHIC is obtained. The predictions up to the LHC energies are made and compared to experimental extrapolations.

Keywords: multihadron production, nuclear collisions, participants, constituent quark

PACS: PACS numbers: 25.75.-q, 24.85.+p, 13.85.-t, 24.10.Nz, 13.66.Bc

1. High densities and temperatures of nuclear matter reached at RHIC provide us with an exceptional opportunity to investigate the matter at extreme conditions. Bulk observables such as multiplicity and particle densities (spectra) being sensitive to the dynamics of strong interactions, are of fundamental interest. Recent measurements at RHIC revealed striking evidences in the hadron production process including similarity in such basic observables like the mean multiplicity and the midrapidity density measured in complex ultra-relativistic nucleus-nucleus (AA) collisions vs. those obtained in relatively “elementary” e^+e^- interactions at the same centre-of-mass (c.m.) energy when number of participants (“wounded” nucleons [1] in AA collisions) are taken into account [2, 3]. The observation is shown to be independent of the c.m. energy per nucleon $\sqrt{s_{NN}} = 19.6$ GeV to 200 GeV. Assuming similar mechanisms of hadron production in both types of interactions which then depends only on the amount of energy transformed into particles produced, one would expect the same value of the observables to be obtained in hadron-hadron collisions at close c.m. energies. However, this is not the case: comparing measurements in hadronic data [4, 5] to the findings at RHIC, one obtains [2, 6, 7] quite lower values in hadron-hadron collisions. In the meantime, the RHIC dAu data at $\sqrt{s_{NN}} = 200$ GeV unambiguously point to the values of the mean multiplicity from $\bar{p}p$ data [2]. Moreover, recent CuCu RHIC data show no changes in the values of the bulk variables compared to those from AuAu collisions when properly normalised to the number of participants [8, 9].

The observations made earlier [2] and the recent ones [9] can be understood in the framework of a description proposed recently by us [10] and considered here. This description is based on a picture when the whole process of a collision is interpreted as the expansion and break-up into particles of an initial state, in which the whole available

energy is assumed to be concentrated in a small Lorentz-contracted volume. There are no any restrictions due to the conservation of quantum numbers besides energy and momentum constraints allowing therefore to link the amount of energy deposited in the collision zone and features of bulk variables in different reactions. This description resembles the Landau hydrodynamical approach to multiparticle production [11] which has been found to give good description of the mean multiplicity AA, pp, e^+e^- , vp data [12, 13] as well as of pseudorapidity distributions at RHIC [6].

As soon as a collision of two Lorentz-contracted particles leads to the full thermalization of the system before extension, one can assume that the production of secondaries is defined by the fraction of participants energy deposited in the volume of the system at the collision moment. This implies that there is a difference between results of collisions of structureless particles like electron and composite particles like proton, the latter considered to be built of constituents. Indeed, in composite particle collisions not all the constituents deposit their energy when they form the Lorentz-contracted volume of the thermalized initial state. As a result, the leading particles [14], formed out of those constituents which are not trapped in the interaction volume, carry away a part of energy. Meantime, colliding structureless particles are ultimately stopped as a whole in the initial state of the thermalized collision zone depositing their total energy in the Lorentz-contracted volume and this energy is wholly available for production of secondaries.

We consider a single nucleon as a superposition of three constituent quarks due to the additive quark picture [15]. In this picture, most often only one quark from each nucleon contributes to the interaction with other quarks being spectators. Thus, the initial thermalized state is pumped in only by the energy of the interacting single quark pair and, so, only 1/3 of the entire nucleon energy is available for production of secondaries. Therefore, one expects that the resulting bulk variables like the multiplicity and rapidity distributions should show identical features in $\bar{p}p$ collisions at the c.m. energy $\sqrt{s_{pp}}$ and in e^+e^- interactions at the c.m. energy $\sqrt{s_{ee}} \simeq \sqrt{s_{pp}}/3$. Note that for the mean multiplicity, a similar behaviour was found in the beginning of LEP activity [16].

In AA collisions, more than one quark per nucleon interacts due to the large size of nucleus and the long path of interactions inside the nucleus. In central AA collisions, a contribution of constituent quarks rather than participating nucleons seem to determine the properties of produced particle distributions [17]. In headon collisions, the density of matter is almost saturated, so that all three constituent quarks from each nucleon may participate nearly simultaneously in collision depositing their energy coherently into the thermalized zone. Therefore, in the headon AA interactions at $\sqrt{s_{NN}}$ the bulk variables are expected to have the values similar to those from pp collisions at $\sqrt{s_{pp}} \simeq 3\sqrt{s_{NN}}$. This makes the most central collisions of nuclei akin to e^+e^- collisions at $\sqrt{s_{ee}} \simeq \sqrt{s_{NN}}$ in sense of the resulting bulk variables.

2. According to our consideration, in Fig. 1, we compare the c.m. energy dependence of the mean multiplicity in AA and e^+e^- interactions to that in pp/ $\bar{p}p$ collisions at $\sqrt{s_{NN}} = \sqrt{s_{ee}} = \sqrt{s_{pp}}/3$ from a few GeV to 200 GeV. For $\sqrt{s_{ee}} > M_{Z^0}$, we give the multiplicities averaged [31] from the recent LEP data at $\sqrt{s_{ee}} = 130$ GeV and 200 GeV: $23.35 \pm 0.20 \pm 0.10$ and $27.62 \pm 0.11 \pm 0.16$. Figure shows also the mean multiplicity fit to pp/ $\bar{p}p$ data [20] and the 3NLO pQCD [33] ALEPH fit to e^+e^- data [27].

From Fig. 1 one sees that the pp/ $\bar{p}p$ data are very close to the e^+e^- data at $\sqrt{s_{ee}} =$

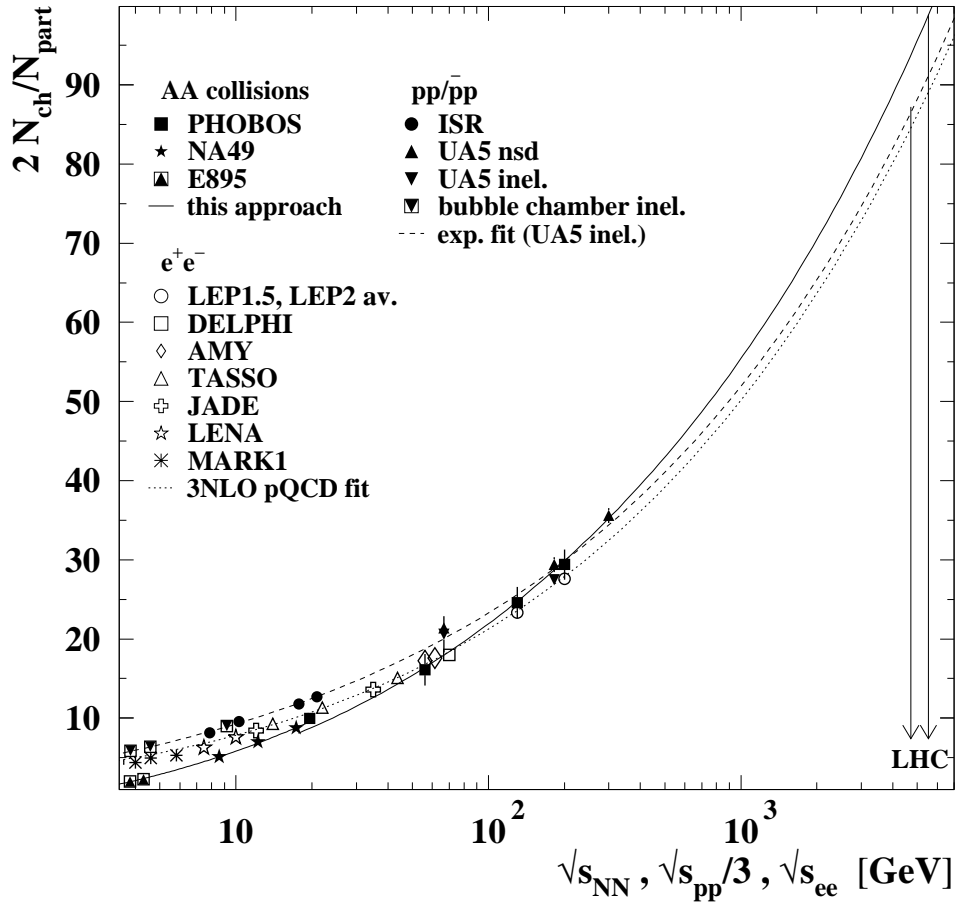


FIGURE 1. The charged particle mean multiplicity N_{ch} per participant pair ($N_{part}/2$) as a function of the c.m. energy. The solid and combined symbols show the multiplicity values from: most central heavy-ion (AA) collisions vs. c.m. energy per nucleon, $\sqrt{s_{NN}}$, measured by PHOBOS [2] (■), NA49 [18] (★), and E895 [19] (▲) (see also [2]); $p\bar{p}$ collisions, by UA5 (▲ for non-single diffractive, ▼ for inelastic events) at $\sqrt{s_{pp}} = 546$ GeV [20] and $\sqrt{s_{pp}} = 200$ and 900 GeV [21]; pp collisions (at lower $\sqrt{s_{pp}}$) from CERN-ISR (●) [22] and bubble chamber experiments [23, 24] (◼) (the latter compiled and analysed in [25]). The inelastic UA5 data at $\sqrt{s_{pp}} = 200$ GeV is due to the extrapolation in [2]. The open symbols show the e^+e^- measurements: the high-energy LEP mean multiplicities (○) averaged here from the data at LEP1.5 $\sqrt{s_{ee}} = 130$ GeV [26, 27] and LEP2 $\sqrt{s_{ee}} = 200$ GeV [27, 28], and the lower-energy data by DELPHI [29] (□), TASSO (△), AMY (◇), JADE (+), LENA (☆), and MARK1 (*) experiments. (See refs. in [30, 31, 32] for e^+e^- and $pp/\bar{p}p$ data). The solid line shows the calculations from Eq. (2) based on our approach and using the corresponding fits (see text). The dashed and dotted lines show the fit [20] to the $pp/\bar{p}p$ data and the 3NLO perturbative QCD [33] ALEPH fit [27] to e^+e^- data. The arrows show the LHC expectations.

$\sqrt{s_{pp}}/3$. This nearness decreases the already small deficit in the e^+e^- data as the energy increases. The deviation can be attributed to the inelasticity factor, or leading particle effect [14] in $pp/\bar{p}p$ collisions, which is known to decrease with the c.m. energy. Then, at lower $\sqrt{s_{pp}}$, some fraction of the energy of spectators contributes more into the formation of the initial state as the spectators pass by. This leads to the excess of the mean multiplicity in $pp/\bar{p}p$ data compared to the e^+e^- data as it is seen in Fig. 1. Comparing further the average multiplicities from $pp/\bar{p}p$ collisions to those from AA ones, one finds that the data points are amazingly close to each other when the AA data

are confronted the hadronic data at $\sqrt{s_{pp}} = 3\sqrt{s_{NN}}$. The inclusion of the tripling energy factor indeed allows to describe such a fundamental variable as the mean multiplicity *simultaneously* in e^+e^- , pp/ $\bar{p}p$ and central AA collisions for all energies. This shows that the multiparticle production process in headon AA collisions is derived by the energy deposited in the Lorentz-contracted volume by a single pair of effectively structureless nucleons similar to that in e^+e^- annihilation and of quark-pair interactions in pp/ $\bar{p}p$ collisions. Note that an examination of Fig. 1 reveals that not a factor 1/2 is needed to rescale $\sqrt{s_{pp}}$ to match the AA or e^+e^- data as earlier was assumed for the mean multiplicity while recognised to unreasonably shift the e^+e^- data on the pseudorapidity density at midrapidity when compared to the AA measurements [2]. This discrepancy finds its explanation in our consideration, within which the data on *both* the mean multiplicity and the midrapidity density (*vide infra*) are self-consistently matched for different reactions. Let us gain recall a factor 1/3 obtained earlier in [16] for $\sqrt{s_{pp}}$ for the pp mean multiplicity data relative to those from e^+e^- data, similar to our finding.

Fig. 1 shows that the mean multiplicities in different reactions are close starting from the SPS $\sqrt{s_{NN}}$, and become particularly close at $\sqrt{s_{NN}} \gtrsim 50$ GeV. However, at lower energies, the AA data are slightly below the e^+e^- and hadronic data and the nuclear data increase faster with energy than the pp and e^+e^- data do. On the other hand, as the c.m. energy increases above a few tens GeV, the AA data start to overshoot the e^+e^- data and reach the mean multiplicity values from $\bar{p}p$ interactions. From this one concludes on two different energy regions of the multiparticle production in AA reactions. The observations made can be understood in terms of the overlap zone and energy deposition by participants [10]. Due to this, one would expect the differences to be more pronounced in midrapidity densities as discussed below.

3. In Fig. 2, we compare the pseudorapidity densities per participant pair at midrapidity as a function of $\sqrt{s_{NN}}$ from headon AA collisions at RHIC, CERN SPS and AGS to those of pp/ $\bar{p}p$ data from CERN and Fermilab plotted vs. $\sqrt{s_{pp}}/3$. Again one can see that up to the existing $\sqrt{s_{NN}}$ the data from hadronic and nuclear experiments are close to each other being consistent with our interpretation. The measurements from the two types of collisions coincide at $8 < \sqrt{s_{NN}} < 20$ GeV and are of the magnitude of the spread of AA data points at 200 GeV. However, above and below the 8-20 GeV region, there are visible differences in the midrapidity η -density values from AA vs. pp data. These indicate that, in contrast to the mean multiplicity which is a more global observable, the midrapidity density depends on some additional factor. As the densities are measured in the very central η -region, where the participants longitudinal velocities are zeroed, it is natural to assume that this factor is related to the size of the Lorentz-contracted volume of the initial thermalized system determined by participants.

To take into account the corresponding correction, let us consider our picture in the framework of the Landau model which is close to our description. Then, one finds for the ratio of the normalised charged particle rapidity density $\rho(y) = (2/N_{\text{part}})dN_{\text{ch}}/dy$ at the midrapidity value $y = 0$ in AA reaction, ρ_{NN} , to the density ρ_{pp} in pp/ $\bar{p}p$ interaction,

$$\rho_{NN}(0)/\rho_{pp}(0) = 2N_{\text{ch}}(L_{pp}/L_{NN})^{1/2} / (N_{\text{part}}N_{\text{ch}}^{\text{pp}}). \quad (1)$$

Here, N_{ch} ($N_{\text{ch}}^{\text{pp}}$) is the multiplicity in AA (pp/ $\bar{p}p$) collision, $L = \ln[\sqrt{s}/(2m)]$, and m is the participant mass, e.g. the proton mass m_p in AA reaction. According to our interpretation, we compare in the ratio (1) $\rho_{NN}(0)$ to $\rho_{pp}(0)$ at $\sqrt{s_{NN}} = \sqrt{s_{pp}}/3$ and

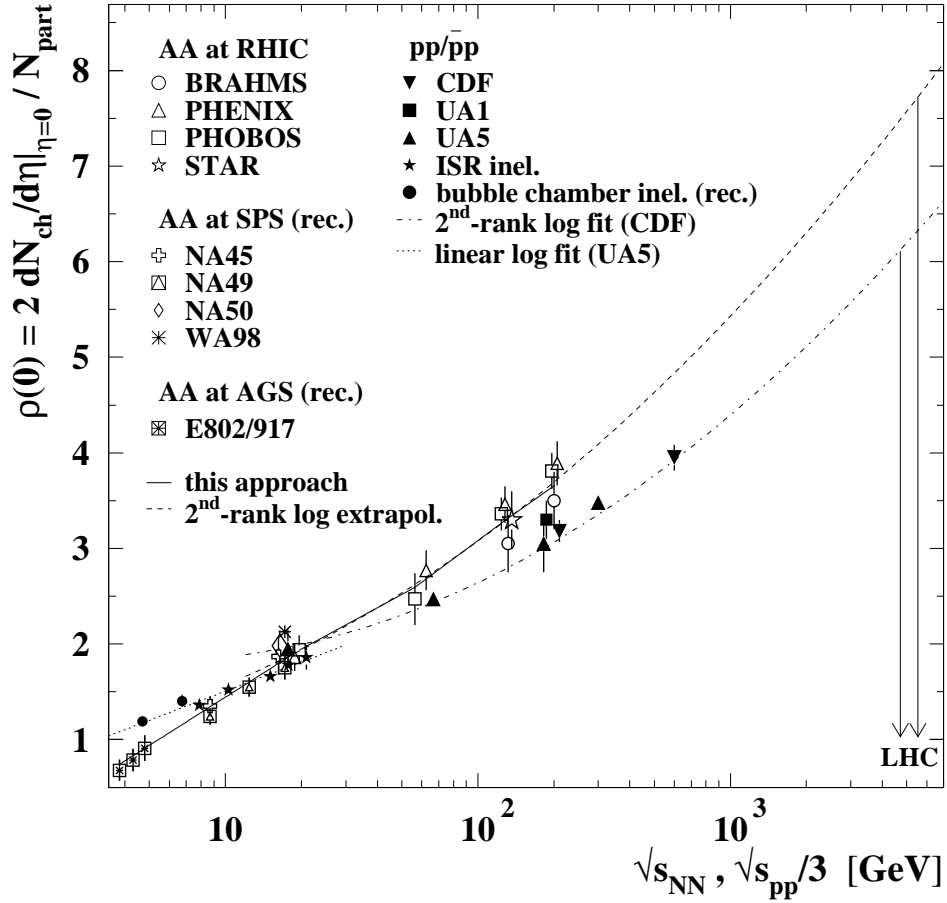


FIGURE 2. Pseudorapidity density $\rho(0)$ of charged particles per participant pair ($N_{\text{part}}/2$) at midrapidity as a function of the c.m. energy of collision. The open and combined symbols show the pseudorapidity density values vs. c.m. energy per nucleon, $\sqrt{s_{\text{NN}}}$, measured in the headon AA collisions by BRAHMS [6] (\circ), PHENIX [7] (\triangle), PHOBOS [2] (\square), and STAR [34] (\star), and the density values recalculated [7] from the measurements taken by CERES/NA45 [35] (\oplus), NA49 [36] (\boxplus), NA50 [37] (\diamond), WA98 [38] (\ast), E802, and E917 [39] (\boxtimes). The nuclear data at $\sqrt{s_{\text{NN}}}$ around 20 GeV and the RHIC data at $\sqrt{s_{\text{NN}}} = 130$ GeV and 200 GeV are given spread horizontally for clarity. The solid symbols show the pseudorapidity density values vs. c.m. energy $\sqrt{s_{\text{pp}}}/3$ as measured in non-single diffractive $\bar{p}p$ collisions by UA1 [40] (\blacksquare), UA5 [4, 20] (\blacktriangle), CDF [5] (\blacktriangledown), and from inelastic pp data from ISR [22] (\star), and bubble chamber [24, 41] (\bullet) experiments (the latter as recalculated in [4]). The solid line connects the predictions from Eq. (2). The dashed line gives the fit to the calculations using the 2nd order log-polynomial fit function analogous to that used [5] in $\bar{p}p$ data. The fit function from [5] is shown by the dashed-dotted line. The dotted line shows the linear log approximation of UA5 to inelastic events [4]. The arrows show the LHC expectations. Note that e^+e^- data at $\sqrt{s_{\text{ee}}} = 14$ GeV to 200 GeV (not shown) follows the heavy-ion data [2].

consider a constituent quark of mass $\frac{1}{3}m_p$ as a participant in $\bar{p}p/\bar{p}p$ collisions and a proton as an effectively structureless participant in headon AA collisions. Then, Eq. (1) reads:

$$\rho_{\text{NN}}(0) = 2N_{\text{ch}}\rho_{\text{pp}}(0) \sqrt{1 - 4\ln 3 / \ln(4m_p^2/s_{\text{NN}})} / (N_{\text{part}}N_{\text{ch}}^{\text{pp}}). \quad (2)$$

Using the fact that the transformation factor from y to η does not influence the above ratio and substituting the multiplicity values from Fig. 1 and of $\rho_{\text{pp}}(0)$ from Fig. 2 into Eq. (2), one obtains the values of $\rho_{\text{NN}}(0)$, displayed in Fig. 2 by solid line. One can see that the correction made provides good agreement between the calculated $\rho_{\text{NN}}(0)$ values

and the data. Eq. (2) shows the importance of the correction for the participant type to be introduced as argued above. One can see that our calculations account also for different types of rise of AA data below and above SPS region. Note that the same two regions recently have been indicated by PHENIX [7] from the ratio of the midrapidity *transverse energy* density to the pseudorapidity density. From these findings, one can expect the midrapidity transverse energy densities in pp/ $\bar{p}p$ and headon AA collisions to be similar due to the description proposed here. Also, the SPS transition region properties discussed by NA49 [18], can be treated without any additional assumptions.

4. To estimate $\rho_{\text{NN}}(0)$ for $\sqrt{s_{\text{NN}}} > 200$ GeV, we extrapolated the values of Eq. (2) utilizing the function found [5] to fit well the $\bar{p}p$ data. The predictions for $\rho_{\text{NN}}(0)$ and the fit for $\bar{p}p$ data are shown in Fig. 2 by dashed and dashed-dotted lines, respectively.

The obtained $\rho_{\text{NN}}(0)$ show faster rise with $\sqrt{s_{\text{NN}}}$ than $\rho_{\text{pp}}(0)$. Our calculations, sharing the behaviour at SPS–RHIC energies with that up to the LHC ones, give $\rho_{\text{NN}}(0) \approx 7.7$ for LHC. From the CDF fit [5] and assuming it covers LHC energies, one finds $\rho_{\text{pp}}(0) \approx 6.1$. Our $\rho_{\text{NN}}(0)$ value for LHC is consistent with that of ≈ 6.1 given in the PHENIX extrapolation [7] within 1-2 particle error acceptable in the calculations we made. Our result is in a good agreement with the best ATLAS Monte Carlo tune [42]. Noticing that $\sqrt{s_{\text{NN}}}$ is near to $\sqrt{s_{\text{pp}}}/3$ at LHC, the close values of $\rho_{\text{NN}}(0)$ and $\rho_{\text{pp}}(0)$, predicted for LHC by us and estimated independently in [7, 42], demonstrates experimentally grounded description and predictive ability of our interpretation.

Solving Eq. (2) for $N_{\text{ch}}/(0.5N_{\text{part}})$ we predict the AA mean multiplicity energy dependence at $\sqrt{s_{\text{NN}}} > 200$ GeV. In this calculations, we use the fits of $\rho_{\text{pp}}(0)$ [5] and $N_{\text{ch}}^{\text{pp}}$ [4] and our approximation for $\rho_{\text{NN}}(0)$, all shown in Figs. 1 and 2. From the resulted curve for $N_{\text{ch}}/(0.5N_{\text{part}})$ given in Fig. 1, one finds that the value obtained for LHC is just about 10% above the $N_{\text{ch}}^{\text{pp}}(\sqrt{s_{\text{pp}}})$ fit [20] prediction for LHC and about 3.3 times larger the AA RHIC data at $\sqrt{s_{\text{NN}}} = 200$ GeV. Again, this number is comparable with the estimate made by [7] and points out to no evidence for change to another regime as the $\sqrt{s_{\text{NN}}}$ increases by about two magnitudes from the top SPS energy. Nevertheless, one can see that the data obtained at the highest RHIC energy give a hint to some border-like behaviour of the mean multiplicity where the pp/ $\bar{p}p$ data saturate the nuclear data, and another transition energy region is possible to be found (as at low energies). This makes AA experiments at $\sqrt{s_{\text{NN}}} > 200$ GeV of particular interest.

5. At the end, let us dwell on the following.

From our description, the mean multiplicity in *nucleon*-nucleus collisions is predicted to be of the same values as that in pp/ $\bar{p}p$ data, and, moreover, almost no centrality dependence is expected for such type of interactions [10]. These predictions are well confirmed by various data from hadron-nucleus collisions at $\sqrt{s_{\text{NN}}} \approx 10$ –20 GeV to recent RHIC dAu data at 200 GeV [2]. The same seems to be correct also for the pseudorapidity density at midrapidity, which is already supported to be a trend [2]. These findings remind about similar conclusions made about two decades ago [12].

The recent observation [8, 9] made at RHIC for multihadron data from CuCu collisions to not change compared to same c.m. energy AuAu data when scaled for the same participant numbers is also understood due to our description as already mentioned. Indeed, for the same number of participants, no difference in the bulk variables is expected as one moves from one type of (identical) colliding nuclei to another one at the same

c.m. energy as soon as the same energy is deposited into the thermalization zone. Note that the proper definition of participants and, thus, of the energy available for particle production, as we discuss here, allows scaling within the constituent quark picture to be applied [8, 17, 43] to model the multihadron data at RHIC for different observables.

One of us (EKGS) is grateful to Organizers for invitation and partial financial support.

REFERENCES

1. A. Białas *et al.*, Nucl. Phys. B **111** (1976) 461; A. Białas, W. Czyż, Acta Phys. Pol. B **36** (2005) 905.
2. B.B. Back *et al.* (PHOBOS), Nucl. Phys. A **757** (2005) 28, and refs. therein.
3. P. Steinberg, J. Phys. G **30** (2004) S683; W. Busza, Acta Phys. Pol. B **35** (2004) 2873.
4. G.J. Alner *et al.* (UA5), Z. Phys. C **33** (1986) 1.
5. F. Abe *et al.* (CDF), Phys. Rev. D **41** (1990) 2330.
6. I. Arsene *et al.* (BRAHMS), Nucl. Phys. A **757** (2005) 1, and refs. therein.
7. K. Adcox *et al.* (PHENIX), Nucl. Phys. A **757** (2005) 184, and refs. therein.
8. R. Noucier, talk at Int. Symp. Multiparticle Dynamics 2005: these Proceedings.
9. G. Roland (for the PHOBOS Collab.), M. Konno (for the PHENIX Collab.): Quark Matter 2005.
10. E.K.G. Sarkisyan and A.S. Sakharov, hep-ph/0410324.
11. L.D. Landau, Izv. Akad. Nauk: Ser. Fiz. **17** (1953) 51.
12. E.L. Feinberg, Proc. Int. Conf. Elementary Particle Physics (Smolenice, 1985), p. 81; Relativistic Heavy Ion Physics (World Scientific, 1991), p. 341.
13. P.A. Carruthers, LA-UR-81-2221 ; P. Steinberg, nucl-ex/0405022.
14. M. Basile *et al.*, Nuovo Cim. A **66** (1981) 129, **73** (1983) 329.
15. V.V. Anisovich *et al.*, Quark Model and High Energy Collisions (World Scientific, 2005).
16. P.V. Chliapnikov and V.A. Uvarov, Phys. Lett. B **251** (1990) 192; for review, see W. Kittel and E.A. De Wolf, Soft Multihadron Dynamics (World Scientific, 2005).
17. S. Eremin and S. Voloshin, Phys. Rev. C **67** (2003) 064905.
18. S.V. Afanasiev *et al.* (NA49), Phys. Rev. C **66** (2002) 054902.
19. J.L. Klay (for the E895 Collab.), PhD Thesis (U.C. Davis, 2001), see [2].
20. G.J. Alner *et al.* (UA5), Phys. Rep. **154** (1987) 247.
21. R.E. Ansorge *et al.* (UA5), Z. Phys. C **43** (1989) 357.
22. W. Thomé *et al.*, Nucl. Phys. B **129** (1977) 365.
23. V.V. Ammosov *et al.*, Phys. Lett. B **42** (1972) 519; C. Bromberg *et al.*, Phys. Rev. Lett. **31** (1974) 254.
24. W.M. Morse *et al.*, Phys. Rev. D **15** (1977) 66.
25. E. De Wolf, J.J. Dumont, F. Verbeure, Nucl. Phys. B **87** (1975) 325.
26. G. Alexander *et al.* (OPAL), Z. Phys. C **72** (1996) 191.
27. A. Heister *et al.* (ALEPH), Eur. Phys. J. C **35** (2004) 457; P. Abreau *et al.* (DELPHI), Phys. Lett. B **372** (1996) 172; P. Achard *et al.* (L3), Phys. Rep. **399** (2004) 71.
28. G. Abbiendi *et al.* (OPAL), Eur. Phys. J. C **37** (2004) 25.
29. P. Abreau *et al.* (DELPHI), Z. Phys. C **70** (1996) 179.
30. P.D. Acton *et al.* (OPAL), Z. Phys. C **53** (1992) 539.
31. Particle Data Group, S. Eidelman *et al.*, Phys. Lett. B **592** (2004) 1, and refs. therein.
32. Compilation by O. Biebel, see <http://www.cern.ch/biebel/www/RPP04/>.
33. I.M. Dremin, J.W. Gary, Phys. Rep. **349** (2001) 301, and refs. therein.
34. C. Adler *et al.* (STAR), Nucl. Phys. A **757** (2005) 102, and refs. therein.
35. F. Ceretto (for the CERES/NA45 Collab., G. Agakichiev *et al.*), Nucl. Phys. A **638** (1998) 467c.
36. F. Siklér (for the NA49 Collab., J. Bächler *et al.*), Nucl. Phys. A **661** (1999) 45c.
37. M.C. Abreau *et al.* (NA50), Phys. Lett. B **530** (2002) 43.
38. M.M. Aggarwal *et al.* (WA98), Eur. Phys. J. C **18** (2001) 651.
39. L. Ahle *et al.* (E802), Phys. Rev. C **59** (1999) 2173; B. Back *et al.* (E917), Phys. Rev. Lett. **86** (2001) 1970.
40. G. Arnison *et al.* (UA1), Phys. Lett. B **123** (1984) 108.
41. J. Whitmore *et al.*, Phys. Rep. **10C** (1974) 273.
42. A.M. Moraes, talk given at ATLAS Physics Week (CERN, Nov. 2004).
43. P.K. Netrakanti, B. Mohanty, Phys. Rev. C **70** (2004) 027901; B. De, S. Bhattacharyya, Phys. Rev. C **71** (2005) 024903.